Published in final edited form as:
Peptides. 2007 September ; 28(9): 1688–1699.

GASTROINTESTINAL DYSFUNCTION IN MICE WITH A TARGETED MUTATION IN THE GENE ENCODING VASOACTIVE INTESTINAL POLYPEPTIDE: A Model for the Study of Intestinal Ileus and Hirschsprung's Disease

V Lelievre[1,4], **G Favrais**[1], **C Abad**[4], **H Adle-Biassette**[1,2], **Y Lu**, **PM Germano**, **G Cheung-Lau**[4], **JR Pisegna**[3], **P Gressens**[1], **G Lawson**[5], and **JA Waschek**[4,6]

1 *IFR Paris 7 and INSERM 676, Hopital Robert Debre Paris, France - AP HP, Hopital Bichat-Claude Bernard*

2 *Service d'Anatomie Pathologie, Paris France*

3 *Division of Gastroenterology and Hepatology VA Greater Los Angeles Healthcare System Los Angeles, CA*

4 *Department of Psychiatry, David Geffen School of Medicine, University of California at Los Angeles, USA*

5 *Deparment of Laboratory Animal Medicine, David Geffen School of Medicine, University of California at Los Angeles, USA*

Abstract

In 1970, Drs. Said and Mutt isolated a novel peptide from porcine intestinal extracts with powerful vasoactive properties, and named it vasoactive intestinal peptide (VIP). Since then, the biological actions of VIP in the gut as well as its signal transduction pathways have been extensively studied. A variety of *in vitro* and *in vivo* studies have indicated that VIP, expressed in intrinsic non-adrenergic non-cholinergic (NANC) neurons, is a potent regulator of gastrointestinal (GI) motility, water absorption and ion flux, mucus secretion and immune homeostasis. These VIP actions are believed to be mediated mainly by interactions with highly expressed $VPAC_1$ receptors and the production of nitric oxide (NO). Furthermore, VIP has been implicated in numerous physiopathological conditions affecting the human gut, including pancreatic endocrine tumors secreting VIP (VIPomas), insulin-dependent diabetes, Hirschsprung's disease, and inflammatory bowel syndromes such as Crohn's disease and ulcerative colitis. To further understand the physiological roles of VIP on the GI tract, we have begun to analyze the anatomical and physiological phenotype of C57BL/6 mice lacking the VIP gene. Herein, we demonstrate that the overall intestinal morphology and light microscopic structure is significantly altered in $VIP^{-/-}$ mice. Macroscopically there is an overall increase in weight, and decrease in length of the bowel compared to wild type (WT) controls. Microscopically, the phenotype was characterized by thickening of smooth muscle layers, increased villi length, and higher abundance of goblet cells. Alcian blue staining indicated that the latter cells were deficient in mucus secretion in $VIP^{-/-}$ mice. The differences became more pronounced from the duodenum to the distal jejunum or ileum of the small bowel but, became much less apparent or absent in the colon with the exception of mucus secretion defects. Further examination of the small intestine revealed larger axonal trunks and unusual unstained patches in myenteric plexus. Physiologically, the $VIP^{-/-}$ mice showed an impairment in intestinal transit. Moreover, unlike WT

[6]To whom correspondence should be addressed: James A Waschek.

C57BL/6 mice, a significant percentage of $VIP^{-/-}$ mice died in the first postnatal year with overt stenosis of the gut.

INTRODUCTION

Since its original characterization by Drs. Victor Mutt and Sami Said in the early 1970's, the actions of vasoactive intestinal polypeptide (VIP) on the gastrointestinal (GI) tract have been extensively studied [30]. VIP displays a 28-amino acid sequence highly conserved between species, and belongs to the secretin/glucagon/pituitary adenylyl cyclase-activating peptide (PACAP) family. Among these members, VIP and PACAP are the most closely related peptides in terms of structure, function and signaling.

VIP has been shown to interact with two differentially expressed, high-affinity, polyvalent VIP/PACAP receptors ($VPAC_1$ and $VPAC_2$), and a PACAP-preferring receptor called PAC_1. Its interaction with these receptors triggers a cascade of intracellular events that differ between the cellular and receptor subtypes. However, in peripheral organs including the GI tract, VIP interacts most commonly with $VPAC_1$, but also $VPAC_2$ receptors [31]. VPAC receptors were initially pharmacologically characterized in membrane extracts from intestinal cells [4] and in colonic adenocarcinoma cell lines [14–15]. VIP was also shown to interact with natriuretic receptors [24] and a recently cloned VIP-specific receptor [41] in guinea pig taeniae coli smooth muscle. In addition, immune cells that are intrinsically present, and that infiltrate the tissue in inflammatory conditions, express both VPAC receptor subtypes. PACAP action and PAC_1 expression appear rather limited in this system, but may play an important physiological role in the digestion-related stomach and pancreas [20].

Among the multiple signaling pathways that VIP activates in the GI tract, the cAMP/PKA pathway is the canonical cascade associated with its intestinal secretagogue functions. However, VIP cAMP-dependent, PKA-independent pathway activation of chloride channels also plays a key role in intestinal absorption. VIP also regulates GI smooth muscle function. These actions may be primarily mediated by $VPAC_1$-initiated phospholipase activities (for review, [18]), including PLC, PLD and PLA. Furthermore, numerous studies have highlighted the functional interaction between VIP and nitric oxide (NO) signaling in GI relaxation, through both cAMP and cGMP signaling cascades (for review, [35]).

VIP is highly expressed in certain specialized enteric neurons. In particular, it has been calculated that VIP-positive neurons represent 45% of the submucosal and 20% of the myenteric neurons in rodent intestine, and 40% of the submucosal innervations of the rat small bowel (for review, [8]). VIPergic innervation along the GI tract plays an important role in the mediation of non-adrenergic, non-cholinergic (NANC) inhibition of smooth muscle contraction, facilitating the relaxation phase of peristalsis. In the GI tract, VIP also acts as a prosecretory neurotransmitter. Since 1971, with the initial demonstration by Barbezat and Grossman that intravenous administration of VIP resulted in fluid accumulation in small bowel of dogs [2], its effects on mucus secretion and electrolyte transport have been extensively studied in primary cell cultures isolated from stomach [11] and colonic cell lines [7,28]. Pathophysiological consequences of this key function in intestine are highlighted by the presence of severe electrolytic diarrhea (Verner and Morrison's syndrome) in patients suffering from VIPomas (for review, [13]).

Actions of VIP on physiological and pathological conditions of the GI tract have been extensively studied using various animal models. Among the wide range of GI pathologies in which VIP may be involved, it is notable that VIP receptors are commonly overexpressed in digestive tumors (including pancreatic tumors and colonic adenocarcinoma). VIP was shown to regulate colonic tumor cell proliferation in vitro [17] and radiolabeled VIP analogs have

proven useful as agents to image tumors in vivo [27]. Furthermore, changes in VIP levels have been associated with inflammatory syndromes. That VIP may exert primarily anti-inflammatory actions was illustrated by its beneficial effects in experimental models of inflammatory bowel disease including Crohn's disease [1] and ulcerative colitis [23]. Finally, VIP may also play a role in peristaltic defects as observed in Hirschsprung's Disease, small-bowel obstruction and paralytic ileus [6]. However, direct evidence linking VIP to the etiology of any GI disorder in humans is lacking.

The development of VIP-deficient mice has provided a unique opportunity to assess the normal biological functions of the peptide, and to assess the potential contribution of its loss to GI disorders in humans. Herein, we report selected baseline anatomical and physiological abnormalities in VIP deficient mice relevant to intestinal disorders such as chronic ileus and Hirschsprung's Disease. Our major findings revealed that the morphology of both epithelium and smooth muscles are affected by loss of VIP, with an overall reduction in secretion of mucus from goblet cells and a major increase in thickness of the muscular layers. These modifications were found to be associated with an intestinal transit defect assessed by invasive methods using non-absorbable materials.

METHODS

Animals

VIP deficient mice backcrossed for at least six generations in a C57BL/6 background housed and fed *ad libitum* in a specific pathogen free animal facility were used in the study [5]. . As controls, WT ($VIP^{+/+}$) age-matched mice from the same genetic background were analyzed. All experiments were approved by the Institutional Animal Care Committees.

Anatomical analyses of gut overall structure

All mice examined in this study were sacrificed by carbon dioxide inhalation. Animals were then weighed and autopsied with systematic analysis of organs weights and potential pathologies. The intestine from the stomach to the rectum was rinsed three times with PBS, prior to fixation with 10% formalin. Cross-sections of the duodenum, proximal, mid and distal jejunum, ileum, proximal, mid and distal colon were collected based on anatomical characteristics. All sections were embedded in paraffin and 5μm sections were cut and stained with hematoxylin and eosin (H&E) (Pathology Inc., Torrance, CA). Sections were observed on a Zeiss microscope and pictures were taken with a 5M pixels digital camera (evolutionMP, Mediacybernetics). Morphometric analyses performed using Q-capture Pro software.

Histological and immunohistological studies

To further analyze differences observed in gut structures in WT vs. $VIP^{-/-}$ animals, periodic acid-schiff (PAS) and Alcian blue stainings were performed using standard procedures on 7μm sections to visualize mucous-secreting cells in both colon and duodenum. In addition, immunostainings to reveal the presence of Schwann cells and axons were performed using S100β, raised in rabbit against a purified bovine S100β (Swant), and pan-neurofilament (NF), raised against a highly purified bovine 150 KD NF peptide (AB1981, Chemicon), respectively. Sections were deparaffinized, rehydrated, and incubated with blocking solution (PBS supplemented with 4% triton X100 and 10% goat serum) for 45 min, prior to primary antibodies (1/1,000 and 1/1,600, respectively). Slides were then rinsed twice with PBS and incubated with HRP-conjugated anti-rabbit IgG goat serum for 45 min according to the original protocol (ABC Vectastain kit) for S100β or with a goat, anti-rabbit IgG conjugate labeled with Fluoprobes 488 dye (FT-FN291, Interchim) for NF, at the working dilution of 1/400. After washes with PBS, sections were directly mounted after serial dehydration in Pertex™ solution for NF labeling or incubated with H_20_2 for 45 s for HPRT staining. Pictures were taken at x40

magnification either on Zeiss light microscope equipped with a 5M pixels digital camera (evolutionMP, Mediacybernetics) or on a Leica fluorescent microscope using an Apogee™ LCD digital camera.

Gastrointestinal motility

Two different methods using non-absorbable boluses were used:

Charcoal gum protocol—Two-month-old female mice (7 wild-type, 9 $VIP^{-/-}$) were previously fasted for 24h (water ad lib.). Gavage on lightly-anaesthetized animals was performed with 200μl of a freshly prepared mixture of gum tragacanth and charcoal (4%/7.5%, respectively) in water. Mice were euthanized 30 min after recovery from anesthesia. GI tracts were dissected and carefully placed on a flat surface. The bolus was easily visualized through the intestinal wall by the black taint of charcoal. Distance from stomach to the most downstream trace of charcoal was measured.

Fluorescein-labeled dextran protocol—Transit through the stomach and intestine was measured in $VIP^{-/-}$ mice and WT controls by evaluating the location of fluorescein-labeled dextran (MW 70 kDa) in the GI tract. After fasting overnight, mice were lightly anesthetized with isoflurane and then gavaged with 150μl of fluorescein-labeled dextran dissolved in distilled water (5 mg/ml). Sixty minutes later, the animals were sacrificed with an overdose of sodium pentobarbital. The entire GI tract from stomach to distal colon was excised and divided into stomach, 10 segments of small intestine with equal length, cecum, proximal colon and distal colon. Dissection of the gut and division into segments were performed carefully with minimal pulling to avoid moving of the gut contents. The content of each segment was collected into a small tube with 1 ml of distilled water. The samples were vortexed and then clarified by centrifugation. The fluorescence of the cleared supernatant from each bowel segment was read at excitation wavelength of 494 nm and emission wavelength of 521 nm. A mean histogram of the fluorescence was then plotted for analysis of transit. The transit of fluorescein-labeled dextran along the GI tract was summarized by calculating the geometric center (GC) using the following formula: GC = (percentage of total fluorescent signal per segment × segment number)/100.

RESULTS

$VIP^{-/-}$ animals show gross anatomical abnormalities in the gastrointestinal tract

Autopsy performed on healthy adult animals revealed obvious anatomical differences in the intestinal tract of knock-out (KO) vs. WT mice. Investigators blind to the genotype could easily distinguish a WT from KO mouse due to rubbery appearance of the gut in $VIP^{-/-}$ mice. In addition, as visualized in Figure 1, an overall reduction in intestinal length was observed in VIP-deficient mice. This difference was noticeable in heterozygous mice, but was more pronounced in KO animals. In addition, we observed a very interesting anatomical abnormality in small bowel (black arrows) associated with degenerated appendices (arrowhead). The weight and density of the small intestinal was found to be greater, but the length reduced in $VIP^{-/-}$ mice (Tables I and II), providing a possible explanation for the ‘rubbery’ phenotype

Differential changes in small bowel and colon light microscopic structure

Detailed morphometric analyses were on performed on histological sections of different parts of the gut, including duodenum, jejunum and ileum for the small bowel and the three sections (ascending, transverse and descending) of the colon. Results are shown in Table III (see the schematic small bowel section in Fig. 1B for structure identification and measurements). Overall, an increase of the cross sectional diameter of the gut sections was observed throughout the small intestine. However, this phenomenon tended to decrease in the small bowel from

140% of the control in duodenum, 128% in proximal jejunum, and 120% in distal jejunum to a non-significant 110% in ileum. The increases in diameter were associated with an increase in the length of villi. These tended to completely fill the lumen of the duodenum, as easily observed in Figure 2A (vs. 2B). At the cellular level, an increase in enterocytic height in VIP-deficient mice was also observed (Table III).

In addition, a significant increase in thickness of the muscularis propria was observed (Figure 2D & F and Table III). This increase in thickness primarily affected the inner (circular) layer. For example, the thickness of the inner layer was almost double in distal jejunum in $VIP^{-/-}$ animals when compared to controls, whereas the thickness of the outer (longitudinal) layer was increased by only 20%. This striking observation is obvious from the pictures presented in Figure 2A–F, but to some extent differentially affected the various parts of the small intestine, with an increased severity in the jejunum, when compared to the duodenum or large intestine (Figures 2E vs. 2F and 3C vs. 3D).

We also investigated the colon of $VIP^{-/-}$ mice for anatomical differences. Unlike that observed in the small intestine, VIP-deficient mice did not appear significantly different to WT mice with respect to villus architecture or smooth muscle thickness (Figure 3, left vs. right panels). Only small differences were observed (Table III), however, these were not consistently seen at all levels of the colon.

Evidence of dysfunctions in goblet cell mucus secretion in $VIP^{-/-}$ animals

Because VIP has long been considered to be a prosecretory neuropeptide, we also focused on the histology of goblet cells in both small and large bowels. In small intestine, we observed a significant increase of the number of mucus-secreting cells in jejunum and ileum in VIP KO mice (Table III). This increase in cell number was associated with a robust increase in the average diameter of the mucus vacuoles of the cells (Table III). The latter is easily observable on HE-stained sections, as shown on figures 2G vs. 2H from proximal jejunum. These differences were further confirmed by selectively labeling mucus using PAS (data not shown) and Alcian blue staining (Figure 4A–D). Alcian blue staining demonstrated mucus accumulation inside the goblet cells in VIP KO mice, correlated with a lack of mucus deposits within the lumen of the duodenum (Figure 4C vs. 4D). The number of goblet cells could not be accurately assessed in colon using H&E (Figures 3C vs. 3D) and specific PAS stainings (data not shown), because of their extremely high abundance.

Effects of VIP on submucosal and myenteric neural innervations

VIP is expressed within neurons of the myenteric plexus, located between the outer longitudinal and inner circular muscle layers of the muscularis propria, and in neurons in the submucosal plexus, located between the submucosa and lamina propria. To determine if loss of VIP affected their anatomical structure, we examined the light microscopic appearance of these plexuses in both small and large intestine. These studies revealed unusual large H&E-negative negative patches within the myenteric and submucosal plexus (Figures 5A vs. 5B) in VIP KO but not WT mice. These patches did not react with the Schwann cell S100β antibody (Pictures C vs. D). In an attempt to further characterize these unstained patches we incubated duodenal sections with fluorescent antibody directed against pan-NF to test whether these patches corresponded to enlarge nerve trunks. This procedure failed to highlight these particular structures, but revealed instead the presence of thicker and brighter axons on sections from VIP-deficient animals (Figures 5E vs. F), suggesting the presence of hypertrophied axons. H&E (Figure 5, G vs. H) and S100 immunostaining (Figure 5, I vs. J) of colonic sections failed to reveal similar differences in large bowel.

Impaired gastrointestinal transit and incidence of early death in VIP-deficient animals

Motility in the upper part of the GI tract was examined in fasted WT and VIP-deficient mice using two different methodologies. In the first of these, charcoal stained gum tragacanth was used as a bolus. This experiment revealed that $VIP^{-/-}$ animals displayed a significant reduction in motility. Indeed, when animals were sacrificed 30 minutes after feeding, we observed an overall 36% decrease ($p=0.0002$) in bolus distance in VIP-deficient mice when compared to controls (Figure 6A). In the second experiment, we used a fluorescent dextran methodology in which the concentration of fluorescent intensity was determined along the length of the intestine. Based on our previous experience with this model, we sacrificed the mice one hour after the beginning of the experiment. As shown in Figure 6B, there was a significant reduction in intestinal transit time in the $VIP^{-/-}$ mice compared to WT mice. Peristalsis and fixed time analysis revealed significant differences in motility pattern indicating that the lack of VIP and associated microscopic abnormalities were reflected in a functional change in motility.

Day to day monitoring of our $VIP^{-/-}$ animal colony in our specific pathogen-free facility revealed that approximately 10–15% of VIP-deficient mice experienced sudden death before the age of twelve months, whereas less than 2% of the wild-type mice in the colony expired during the same period. Origins of these early deaths were difficult to elucidate because of the short time window allowing the autopsy of the carcasses to be performed prior to autolysis. Nonetheless, an abrupt blockade in movement of intestinal contents was observed in most of these mice, as revealed by a gross swelling of the intestine at all levels above an apparent stricture. In a few cases, we were able to euthanize before they had succumbed. H&E stained sections did not reveal physical block or inflammatory infiltrates, or any obvious pathology except for typical GI stenosis (data not shown). These findings suggested that the early death in these mice was due to stenosis of the gut.

DISCUSSION

VIP was first characterized as a peptide expressed in the intestine and the lung, but was later found to be widely expressed in the central and peripheral nervous systems. A wide variety of experimental approaches indicate that this peptide acts as a neurotransmitter or neuromodulator in the brain and nearly all peripheral systems, including cardiovascular, reproductive, and immune systems. We report here the first description of the GI phenotype of mice deficient in this peptide. While some of the anatomical findings were unexpected, functional studies revealed that GI motility was impaired in $VIP^{-/-}$ mice, a finding fully in line with studies showing that this peptide acts in the gut as a smooth muscle relaxant. Moreover, the ratio of goblet cell-retained vs. secreted mucus was higher in VIP KO mice, suggesting a pro-secretory role for VIP in goblet cells, another finding in accordance to considerable work of others.

The most obvious anatomical alteration in VIP KO mice was that the intestine was heavier but shorter compared to WT controls. The higher density was reflected in an increased luminal diameter at several levels of the GI tract, especially in the duodenum and jejunum portions of the intestine. Part of the increased diameter could be accounted for by a thickening of both the outer longitudinal and inner circular layers of the muscularis propria. Some peculiar findings were that VIP-deficient mice exhibited increases in the mean enterocyte length (basal to serosal) and villus length.

A possible explanation for the decreased length and increased thickness of the bowel is that the intestine might have been in a relatively enhanced state of tonic contraction. However, this mechanism cannot account for the substantial increase in overall mass of the small intestine (>60%, see Table I). This increased mass could be triggered in some way in response to the impaired GI function in VIP KO mice. Another possibility is that some of the changes are due to a developmental loss of VIP. In this regard, VIP has been shown to exhibit growth factor-

like action in vitro on many different types of primary cells and tumor cell lines (reviewed in [22,36–37]. With respect to the intestine, VIP has been shown to regulate the proliferation of intestinal epithelial cells [32–34] and cell lines [10,17,40]. This peptide might also regulate intestinal smooth muscle proliferation, because VIP was show to inhibit the proliferation of vascular smooth muscle [19]. In this regard, we recently showed that $VIP^{-/-}$ mice exhibit pulmonary hypertension with thickening of the smooth muscle layers in the pulmonary artery and smaller branches [29].

The possibility that VIP acts a growth factor in the gut is interesting in light of recent findings that hedgehog proteins regulate GI development [9]. Hedgehog actions are antagonized by cAMP-dependent protein kinase A (PKA). The VIP-related peptide PACAP was shown to inhibit sonic hedgehog-induced proliferation of cultured cerebellar granule precursors [25]. The growth factor-like actions of VIP and PACAP raise the possibility that these peptides have significance in intestinal tumor pathogenesis. In this regard, VIP and PACAP have been shown to modulate proliferation of adenocarcinoma cell lines [17] and VIP levels are enhanced in serum samples from patients suffering from colonic carcinoma [12]. The interaction with the hedgehog pathway might also be relevant in these tumors because the hedgehog pathway has been found to be overactive in human intestinal carcinomas [3] and associated with tumor cell survival [26]. In these respects, VIP-deficient mice may be a useful model to study the role of the endogenous peptide in the pathogenesis and/or progression of intestinal tumors.

An appealing extrapolation of the present results is to link the observed phenotypes with major human digestive disorders. Among the characteristic GI features observed in $VIP^{-/-}$ animals was small bowel dilatation and muscular hypertrophy associated with an apparent reduction of peristalsis. Thus, mice lacking VIP-ergic innervation might represent a model for human pathologies characterized by peristaltic defects, for example Hirschsprung's disease, or children with constipation associated with clinical symptoms of intestinal pseudo-obstruction. The potential clinical relevance of this comparison is reinforced by the observation of lethal duodenal stenosis in $VIP^{-/-}$ animals and by analogies in clinical features previously observed in a rat model for long segment Hirschsprung's disease [38]. Furthermore, while a reduction in VIP innervation has been reported in these pathologies (for review, [16]), it is still quite unclear whether reduction in VIPergic innervation is indeed causative or resultant in the disease progression. In addition, the unusual spotted plexuses observed in $VIP^{-/-}$ animals may in fact correspond to the increase in nerve trunks in the muscularis propria previously reported from biopsies of patients suffering from Hirschsprung's disease [21]. Moreover, as speculated above, interactions between VIP and hedgehog pathway might also play a role the generation of Hirschsprung's-like phenotype in mice, since overexpression of human gli1 gene in transgenic mice triggered patches of GI dilatation [39].

In conclusion, the present data represent the first direct evidence that VIP has an endogenous effect on digestive function and GI tract integrity. Additional work is necessary to fully describe the overall digestive phenotype observed in VIP null mice and understand the relationship between lack of VIP and GI disorders. These studies provide an insight into the pathogenesis of intestinal motility abnormalities in humans and provide an experimental model to study intestinal ileus, pseudoobstruction (Oglievie's Syndrome) and Hirschsprung's disease.

Acknowledgements

G. Favrais was recipient of fellowships from the French Society for Pediatrics and the Evian's Foundation. J. Waschek received a pilot award from the Center of Ulcer Research and Education (CURE), and was funded by HD0657 and HD34475. JR Pisegna was funded by the Department of Veterans Affairs. PM Germano was funded by an NIDDK NIH Re-entry grant program.

References

1. Abad C, Martinez C, Juarranz MG, Arranz A, Leceta J, Delgado M, Gomariz RP. Therapeutic effects of vasoactive intestinal peptide in the trinitrobenzene sulfonic acid mice model of Crohn's disease. Gastroenterology 2003;124:961–71. [PubMed: 12671893]
2. Barbezat GO, Grossman MI. Intestinal secretion: stimulation by peptides. Science 1971;174:422–4. [PubMed: 5111998]
3. Berman DM, Karhadkar SS, Maitra A, Montes De Oca R, Gerstenblith MR, Briggs K, Parker AR, Shimada Y, Eshleman JR, Watkins DN, Beachy PA. Widespread requirement for Hedgehog ligand stimulation in growth of digestive tract tumours. Nature 2003;425:846–51. [PubMed: 14520411]
4. Binder HJ, Lemp GF, Gardner JD. Receptors for vasoactive intestinal peptide and secretin on small intestinal epithelial cells. Am J Physiol 1980;238:G190–6. [PubMed: 6245588]
5. Colwell CS, Michel S, Itri J, Rodriguez W, Tam J, Lelievre V, Hu Z, Liu X, Waschek JA. Disrupted circadian rhythms in VIP- and PHI-deficient mice. Am J Physiol Regul Integr Comp Physiol 2003;285:R939–49. [PubMed: 12855416]
6. Cullen JJ, Caropreso DK, Hemann LL, Hinkhouse M, Conklin JL, Ephgrave KS. Pathophysiology of adynamic ileus. Dig Dis Sci 1997;42:731–7. [PubMed: 9125641]
7. Dharmsathaphorn K, McRoberts JA, Mandel KG, Tisdale LD, Masui H. A human colonic tumor cell line that maintains vectorial electrolyte transport. Am J Physiol 1984;246:G204–8. [PubMed: 6141741]
8. Fujimiya M, Inui A. Peptidergic regulation of gastrointestinal motility in rodents. Peptides 2000;21:1565–82. [PubMed: 11068106]
9. Fukuda K, Yasugi S. Versatile roles for sonic hedgehog in gut development. J Gastroenterol 2002;37:239–46. [PubMed: 11993506]
10. Gamet L, Murat JC, Remaury A, Remesy C, Valet P, Paris H, Denis-Pouxviel C. Vasoactive intestinal peptide and forskolin regulate proliferation of the HT29 human colon adenocarcinoma cell line. J Cell Physiol 1992;150:501–9. [PubMed: 1371513]
11. Hakanson R, Chen D, Lindstrom E, Bernsand M, Norlen P. Control of secretion from rat stomach ECL cells in situ and in primary culture. Scand J Clin Lab Invest Suppl 2001;234:53–60. [PubMed: 11713981]
12. Hejna M, Hamilton G, Brodowicz T, Haberl I, Fiebiger WC, Scheithauer W, Virgolini I, Kostler WJ, Oberhuber G, Raderer M. Serum levels of vasoactive intestinal peptide (VIP) in patients with adenocarcinomas of the gastrointestinal tract. Anticancer Res 2001;21:1183–7. [PubMed: 11396161]
13. Krejs GJ. VIPoma syndrome. Am J Med 1987;82:37–48. [PubMed: 3035922]
14. Laburthe M, Breant B, Rouyer-Fessard C. Molecular identification of receptors for vasoactive intestinal peptide in rat intestinal epithelium by covalent cross-linking. Evidence for two classes of binding sites with different structural and functional properties. Eur J Biochem 1984;139:181–7. [PubMed: 6321173]
15. Laburthe M, Rousset M, Chevalier G, Boissard C, Dupont C, Zweibaum A, Rosselin G. Vasoactive intestinal peptide control of cyclic adenosine 3′:5′-monophosphate levels in seven human colorectal adenocarcinoma cell lines in culture. Cancer Res 1980;40:2529–33. [PubMed: 6248206]
16. Larsson LT. Hirschsprung's disease--immunohistochemical findings. Histol Histopathol 1994;9:615–29. [PubMed: 7981507]
17. Lelievre V, Meunier AC, Caigneaux E, Falcon J, Muller JM. Differential expression and function of PACAP and VIP receptors in four human colonic adenocarcinoma cell lines. Cell Signal 1998;10:13–26. [PubMed: 9502113]
18. Makhlouf GM, Murthy KS. Signal transduction in gastrointestinal smooth muscle. Cell Signal 1997;9:269–76. [PubMed: 9218127]
19. Maruno K, Absood A, Said SI. VIP inhibits basal and histamine-stimulated proliferation of human airway smooth muscle cells. Am J Physiol 1995;268:L1047–51. [PubMed: 7541947]
20. Miampamba M, Germano PM, Arli S, Wong HH, Scott D, Tache Y, Pisegna JR. Expression of pituitary adenylate cyclase-activating polypeptide and PACAP type 1 receptor in the rat gastric and colonic myenteric neurons. Regul Pept 2002;105:145–54. [PubMed: 11959368]

21. Monforte-Munoz H, Gonzalez-Gomez I, Rowland JM, Landing BH. Increased submucosal nerve trunk caliber in aganglionosis: a “positive” and objective finding in suction biopsies and segmental resections in Hirschsprung’s disease. Arch Pathol Lab Med 1998;122:721–5. [PubMed: 9701334]
22. Moody TW, Hill JM, Jensen RT. VIP as a trophic factor in the CNS and cancer cells. Peptides 2003;24 (1):163–77. [PubMed: 12576099]
23. Mourad FH, Barada KA, Bou Rached NA, Khoury CI, Saade NE, Nassar CF. Inhibitory effect of experimental colitis on fluid absorption in rat jejunum: role of the enteric nervous system, VIP, and nitric oxide. Am J Physiol 2006;290:G262–8.
24. Murthy KS, Teng BQ, Zhou H, Jin JG, Grider JR, Makhlouf GM. G(i-1)/G(i-2)-dependent signaling by single-transmembrane natriuretic peptide clearance receptor. Am J Physiol 2000;278:G974–80.
25. Nicot A, Lelievre V, Tam J, Waschek JA, DiCicco-Bloom E. Pituitary adenylate cyclase-activating polypeptide and sonic hedgehog interact to control cerebellar granule precursor cell proliferation. J Neurosci 2002;22:9244–54. [PubMed: 12417650]
26. Qualtrough D, Buda A, Gaffield W, Williams AC, Paraskeva C. Hedgehog signalling in colorectal tumour cells: induction of apoptosis with cyclopamine treatment. Int J Cancer 2004;110:831–7. [PubMed: 15170664]
27. Raderer M, Kurtaran A, Hejna M, Vorbeck F, Angelberger P, Scheithauer W, Virgolini I. 123I-labelled vasoactive intestinal peptide receptor scintigraphy in patients with colorectal cancer. Br J Cancer 1998;78:1–5. [PubMed: 9662242]
28. Rouyer-Fessard C, Augeron C, Grasset E, Maoret JJ, Laboisse CL, Laburthe M. VIP receptors and control of short circuit current in the human intestinal clonal cell line Cl. 19A Experientia 1989;45:1102–5.
29. Said SI, Hamidi SA, Dickman KG, Szema AM, Lyubsky S, Lin RZ, Jiang YP, Chen JJ, Waschek JA, Kort S. Moderate Pulmonary Arterial Hypertension in Male Mice Lacking the Vasoactive Intestinal Peptide Gene. Circulation 2007;15:1260–8. [PubMed: 17309917]
30. Said SI, Mutt V. Polypeptide with broad biological activity: isolation from small intestine. Science 1970;169:1217–8. [PubMed: 5450698]
31. Schulz S, Rocken C, Mawrin C, Weise W, Hollt V, Schulz S. Immunocytochemical identification of VPAC1, VPAC2, and PAC1 receptors in normal and neoplastic human tissues with subtype-specific antibodies. Clin Cancer Res 2004;10:8235–42. [PubMed: 15623599]
32. See NA, Epstein ML, Dahl JL, Bass P. The myenteric plexus regulates cell growth in rat jejunum. J Auton Nerv Syst 1990;31:219–29. [PubMed: 2084186]
33. Simopoulos C, Gaffen JD, Bennett A. Effects of gastrointestinal hormones on the growth of human intestinal epithelial cells in vitro. Gut 1989;30:600–4. [PubMed: 2731751]
34. Toumi F, Neunlist M, Cassagnau E, Parois S, Laboisse CL, Galmiche JP, Jarry A. Human submucosal neurones regulate intestinal epithelial cell proliferation: evidence from a novel co-culture model. Neurogastroenterol Motil 2003;15:239–42. [PubMed: 12787332]
35. Van Geldre LA, Lefebvre RA. Interaction of NO and VIP in gastrointestinal smooth muscle relaxation. Curr Pharm Des 2004;10:2483–97. [PubMed: 15320758]
36. Waschek JA. Vasoactive intestinal peptide: an important trophic factor and developmental regulator? Dev Neurosci 1995;17:1–7. [PubMed: 7621745]
37. Waschek JA. VIP and PACAP receptor-mediated actions on cell proliferation and survival. Ann N Y Acad Sci 1996;805:290–300. [PubMed: 8993411]
38. Won KJ, Torihashi S, Mitsui-Saito M, Hori M, Sato K, Suzuki T, Ozaki H, Karaki H. Increased smooth muscle contractility of intestine in the genetic null of the endothelin ETB receptor: a rat model for long segment Hirschsprung’s disease. Gut 2002;50:355–60. [PubMed: 11839714]
39. Yang JT, Liu CZ, Villavicencio EH, Yoon JW, Walterhouse D, Iannaccone PM. Expression of human GLI in mice results in failure to thrive, early death, and patchy Hirschsprung-like gastrointestinal dilatation. Mol Med 1997;3:826–35. [PubMed: 9440116]
40. Yu D, Seitz PK, Selvanayagam P, Rajaraman S, Townsend CM Jr, Cooper CW. Effects of vasoactive intestinal peptide on adenosine 3′,5′-monophosphate, ornithine decarboxylase, and cell growth in a human colon cell line. Endocrinology 1992;131:1188–94. [PubMed: 1324153]
41. Zhou H, Huang J, Murthy KS. Molecular cloning and functional expression of a VIP-specific receptor. Am J Physiol 2006;291:G728–34.

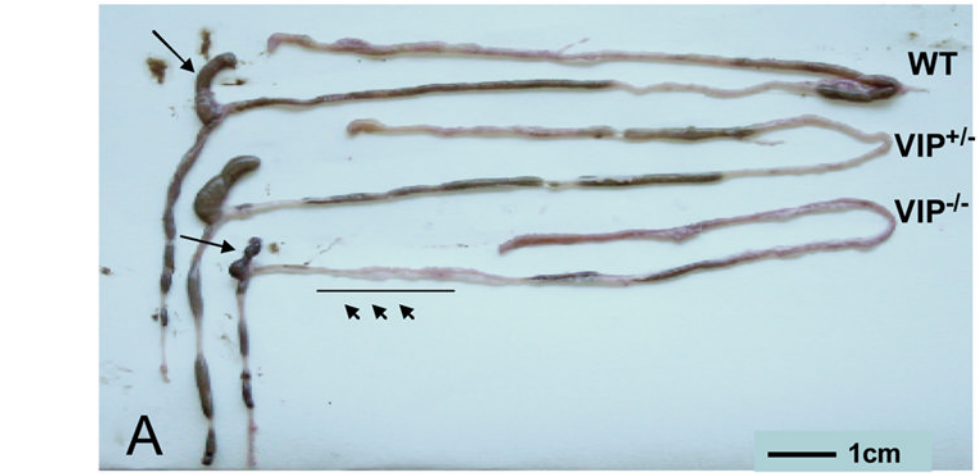

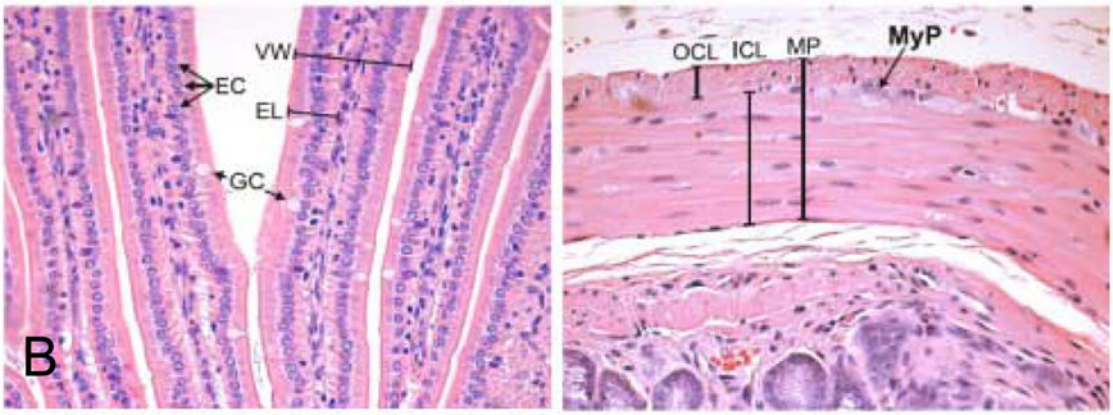

Figure 1.

A: Low magnification picture of the GI tract of representative WT, $VIP^{+/-}$, and $VIP^{-/-}$ mice. Of interest, total GI length and appendix size are reduced when compared to their dimensions in the tract from a representative age-matching control animal B. High magnification photomicrographs showing some of the anatomical details reported in Table III. Left panel shows individual villi: arrows point to enterocytes (EC) and mucous-secreting (goblet) cells (GC); VW- and EL-labeled brackets denote villus width and enterocyte length, respectively. Right panel is a high power view showing the muscularis propria (MP), consisting of the outer (longitudinal) cell layer (OCL) and the inner (circular) cell layer (ICL). Arrow points to a myenteric plexus (MyP), which lies between the two muscle layers of the muscularis propria.

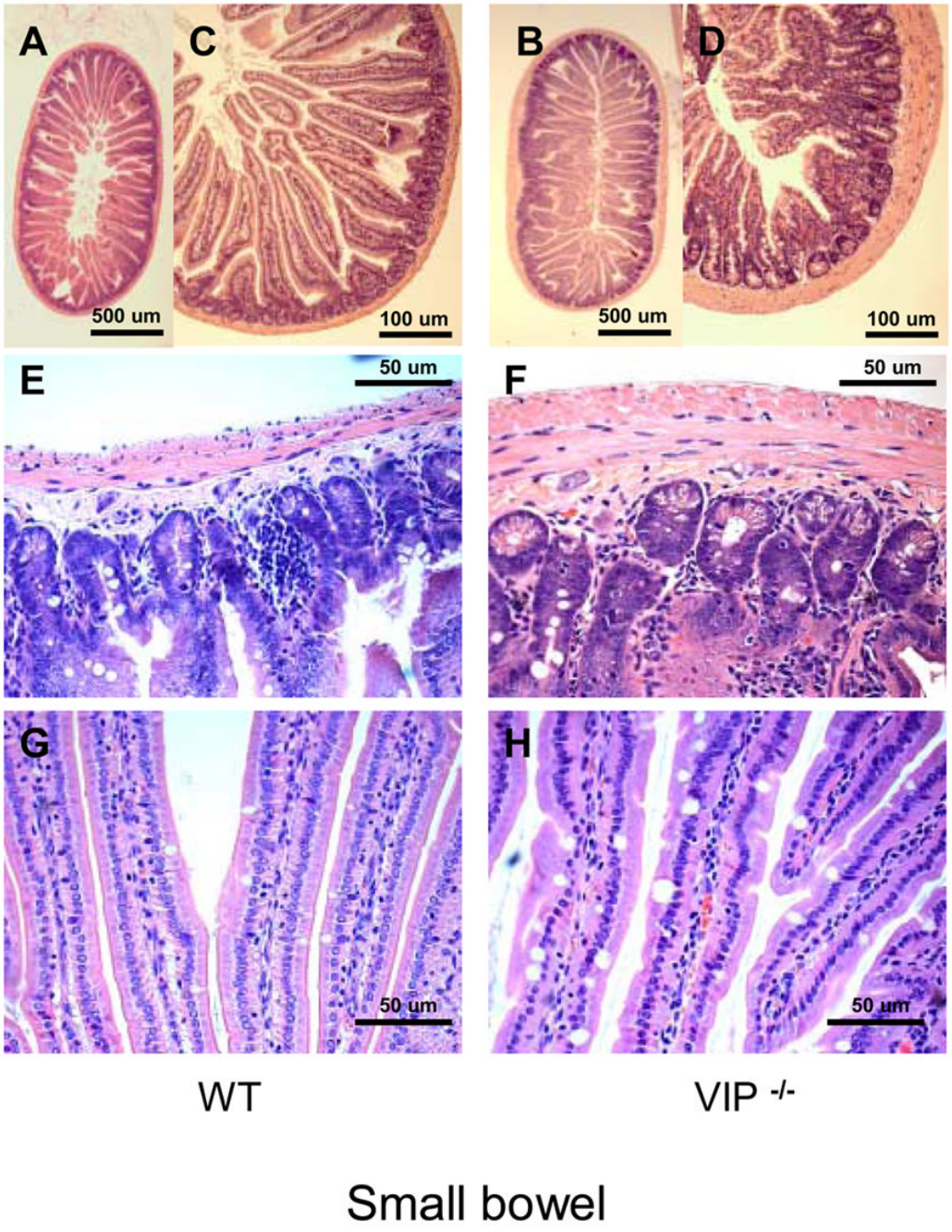

Figure 2.

Microscopic structure of the proximal jejunum in WT and VIP$^{-/-}$ mice. Small bowel sections were stained using standard H&E staining. Pictures at low (x2.5, x10, upper panel) and higher magnification (x20, x40; mid and lower panels, respectively) revealed an overall increase in thickness of muscularis mucosa in VIP KO (B, D and F) vs. controls (A, C and E), as well as higher numbers of mucus-forming cells (G vs. E).

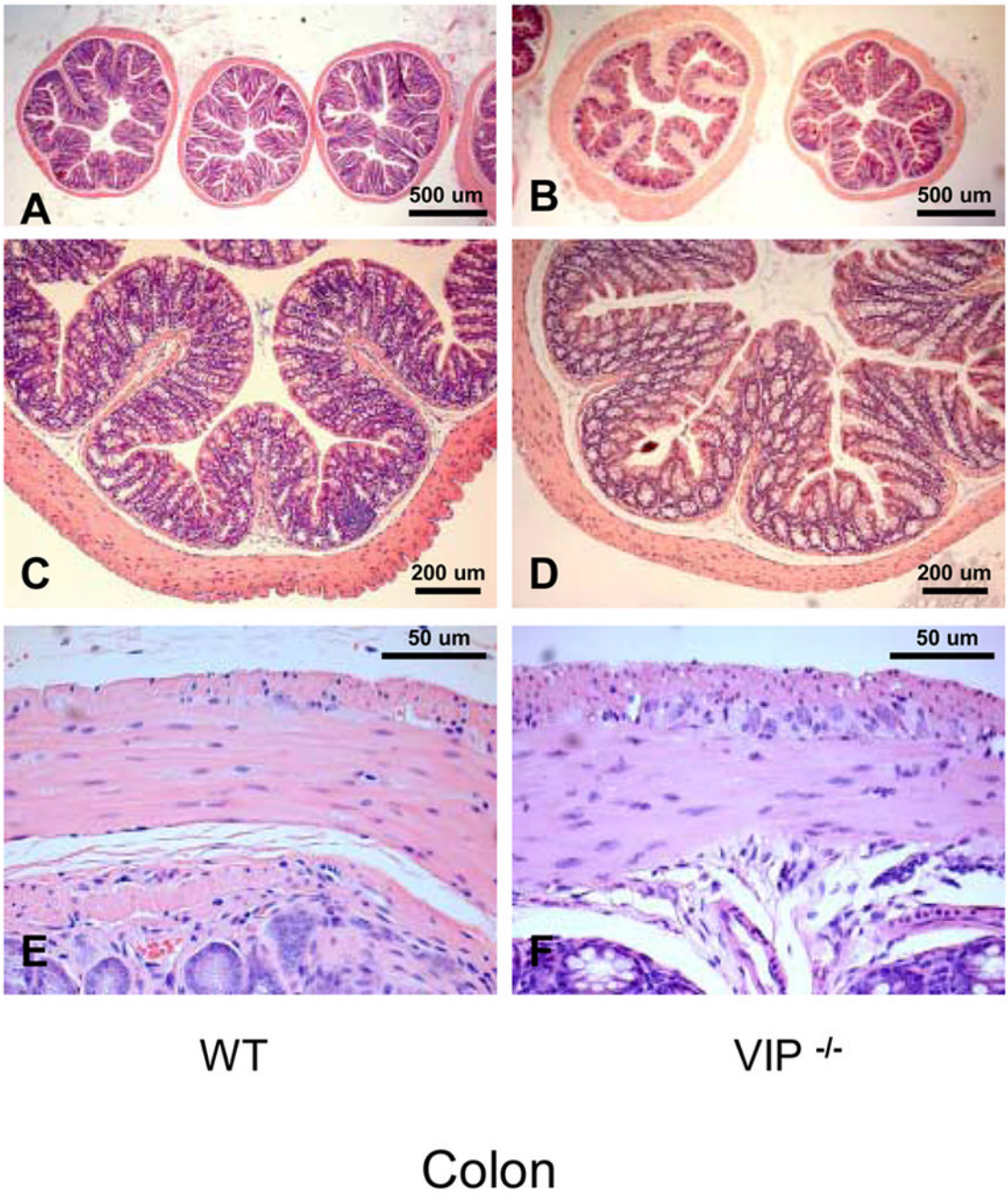

Figure 3.
Microscopic structure of the colon in WT and VIP$^{-/-}$ mice. Gut sections were stained using standard H&E staining.

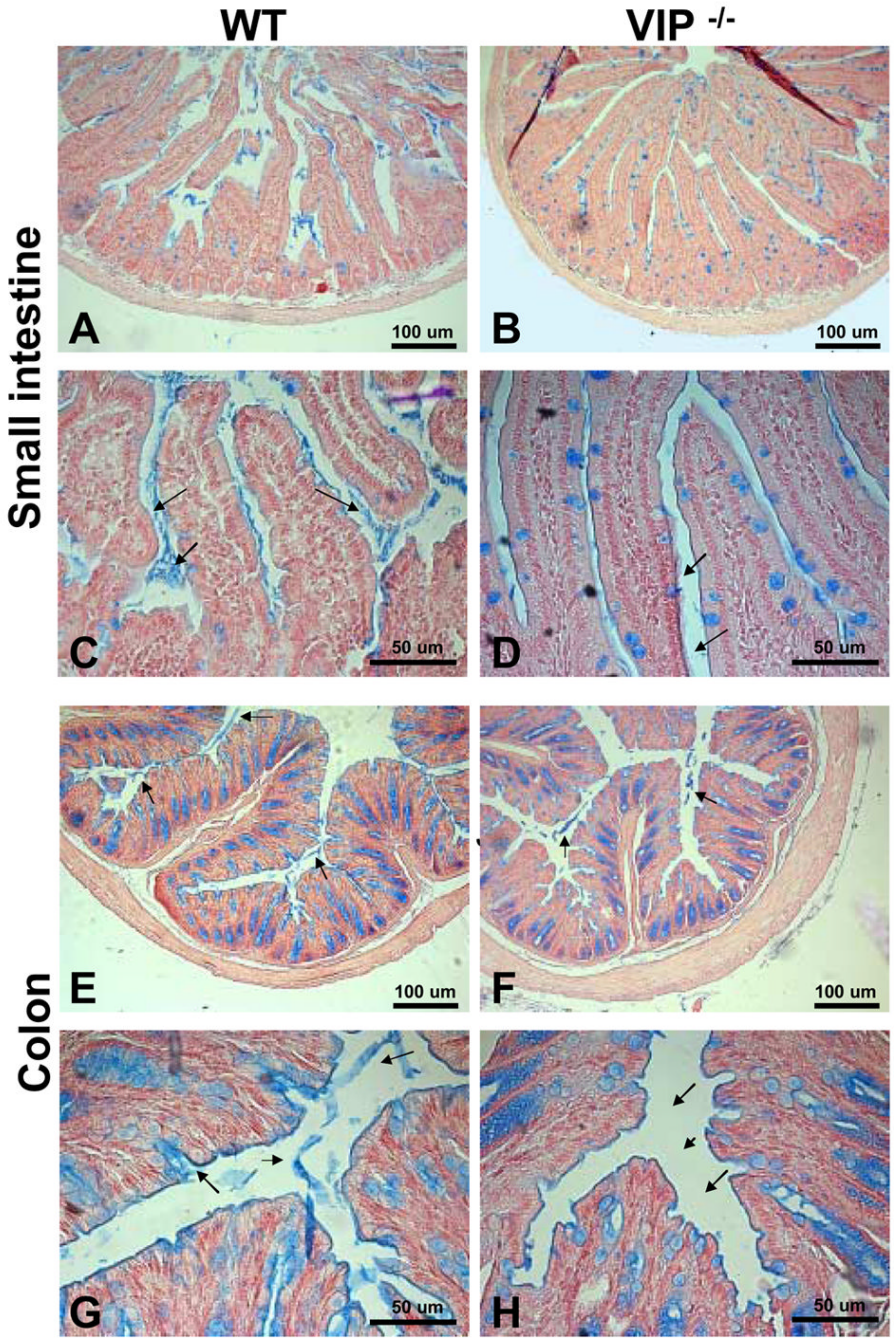

Figure 4.

Alcian blue staining to visualize mucus deposits on sections in duodenum (A–D) and distal colon (E–H) from WT (left panel) and VIP$^{-/-}$ mice (right panels). As expected from H&E staining shown in figures 2 & 3, Alcian blue staining revealed a significant difference in mucus-positive cells in the small intestine, but no change in colon. However, sections from VIP$^{-/-}$ showed a dramatic reduction in the amount of mucus released in the lumen in both small (A, C vs B, D), and large (E, G vs F, H) bowels.

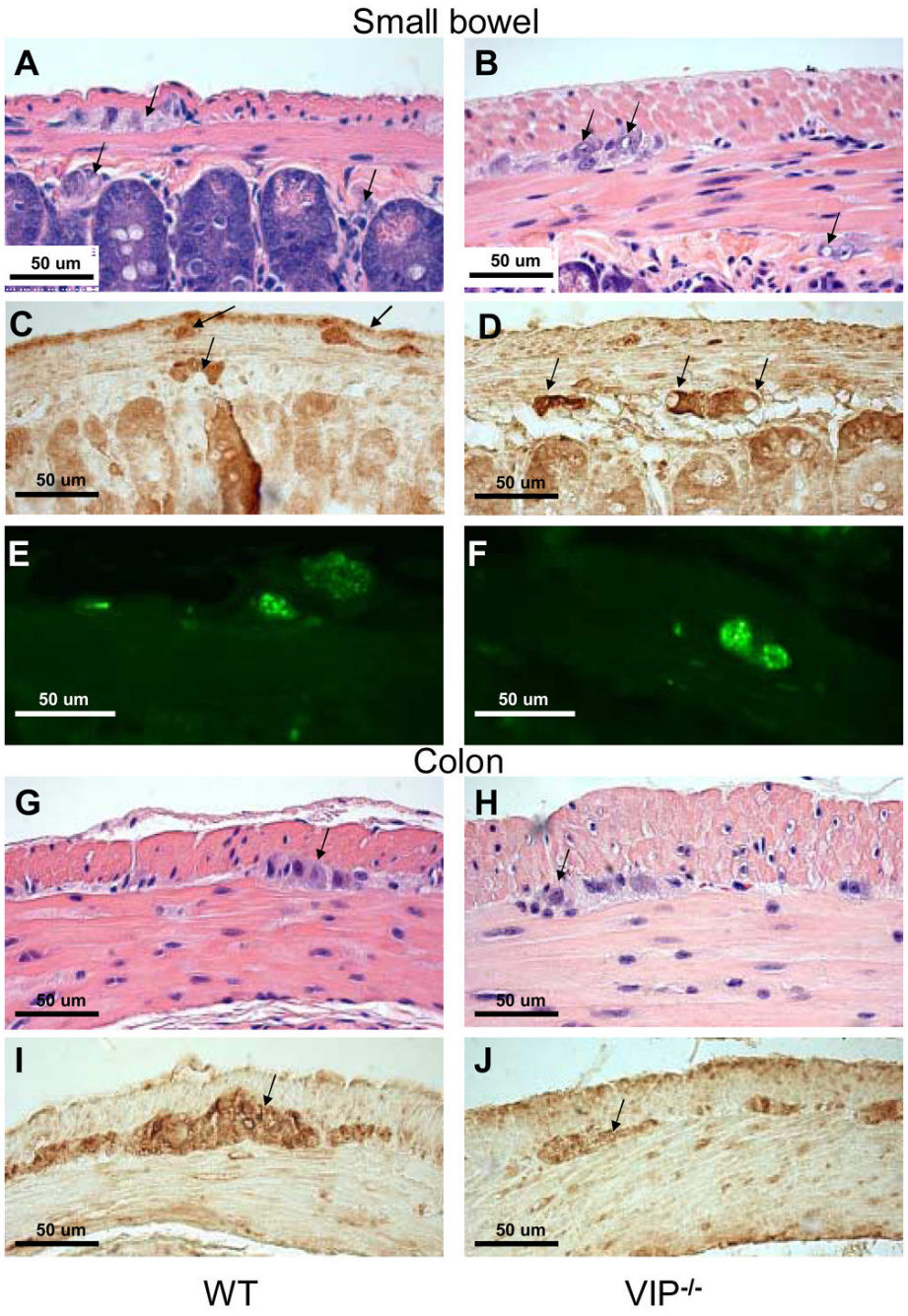

Figure 5.

Microscopic structure of myenteric plexus in duodenum and distal colon of WT and VIP$^{-/-}$ mice. H&E (A, B, G and H) and S100β (C–D & I–J) and pan-neurofilaments (NF) (E, F) stainings are shown in WT and VIP KO mice (left and right panels, respectively). Structural differences were observed in duodenum of VIP deficient mice when compared to WT controls. Plexuses from KO mice showed enlarged unstained patches (A vs B) that were non-immunoreactive with S100β or NF antibodies used to specifically reveal Schwann cells and axons (C vs. D & E vs. F, respectively). However, immunofluorescence emitted by the pan-NF antibody coupled with green fluorescent dye-labeled conjugates (E vs. F) revealed larger area signals within the external plexus of the KO mice than WT controls, suggesting the

presence of bigger axons within the myenteric plexus of VIP-deficient mice. Conversely, no obvious differences in plexus structures of the large bowel (G–J) were using these techniques (pan-NF not shown).

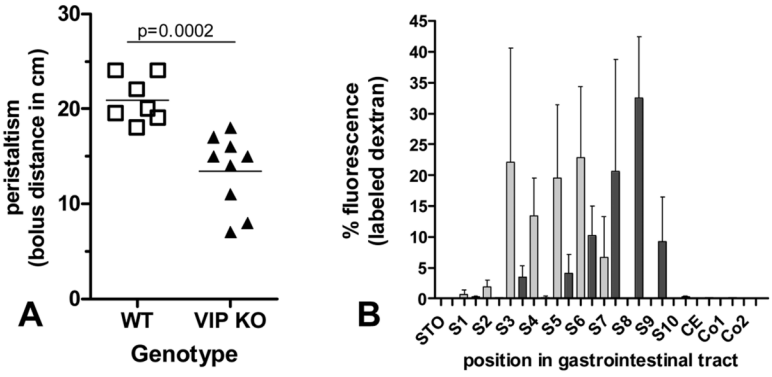

Figure 6.

Peristaltic activity in WT vs. VIP$^{-/-}$ mice. A: migration of charcoal-stained bolus along the GI tract 30 min after gavage. B: Distribution of fluorescein-labeled dextran along the gastrointestinal tract 60 minutes post administration in WT controls vs. VIP$^{-/-}$ mice. Procedures are described in methods. Data are presented as mean ± SEM (n=3).

Table I

Morphometric analyses of digestive organs from VIP KO mice compared to age-matching wild type controls.

Organs	WT	VIP KO
Weight (% of body weight)	4.70 +/− 0.62	4.34 +/− 0.17
Liver	0.98+/− 0.22	1.37+/− 0.15*
Pancreas	0.98+/− 0.18	1.23 +/− 0.13*
Colon	4.31+/− 0.34	7.13 +/− 0.28*
small intestine		
Density (g/cm)	0.036 +/− 0.0021	0.051+/− 0.0016*
Pylorus to colon	0.032 +/− 0.0043	0.067 +/−0.0028*
Colon to rectum		

* Indicates statistically significant differences between VIP KO (n= 8) and control (n= 13) mice; ($p<0.05$).

Table II

Morphometric analyses of intestinal structures in WT and VIP$^{-/-}$ mice. * Indicates statistically significant differences between VIP KO (n= 6) and control mice (n= 5)

Intestinal structures	Measurements (cm +/− SD)		Differences (% of WT control)
	WT	VIP$^{-/-}$	
Length Pylorus to rectum	57.00+/− 0.71	50.25+/−2.72	88.16*
Pylorus to cecum	47.13 +/− 1.03	42.12+/−3.11	89.39
Cecum to rectum	9.88 +/− 0.63	8.00+/−0.72	81.01*
Cecum	2.63 +/− 0.25	3.25+/−0.52	123.81

* p<0.05,

** p<0.01

*** p<0.005

Table III

Systematic comparisons between WT and VIP$^{-/-}$ animals at the levels of small and large intestine. Parameters were determined from histological sections (See Fig. 1B). Du = duodenum, D = distal duodenum, IL = ileum, PC = proximal colon, C = middle colon, DC = distal colon, PJ = proximal jejunum, J = middle jejunum and DJ = distal jejunum. Data were expressed as mean, calculated from 4 to 13 individuals per group (4 measurements/section; 4 sections/animal). P values were determined by Student's t test (ns: non significant). To determine diameters on cross sections, minimal and maximal widths were determined and averaged.

Small intestine	**DU**			**D**			**PJ**			**J**			**DJ**			**IL**		
	WT	**KO VIP**	**p**	**WT**	**KO VIP**	**p**	**WT**	**KO VIP**	**p**	**WT**	**KO VIP**	**p**	**WT**	**KO VIP**	**p**	**WT**	**KO VIP**	**p**
Number of animals (n)	**5**	**6**		**10**	**6**		**9**	**8**		**4**	**4**		**14**	**12**		**13**	**11**	
Average gut diameter (µm)	1755	2428	*<0.0001*	1873	2591	*0.0005*	1801	2292	*<0.0001*	1639	1848	*ns*	1711	2555	*0.006*	1457	1697	*ns*
villus length (µm)	567	681	*0.006*	555	639	*0.008*	498	572	*0.0055*	445	552	*0.02*	340	435	*0.0003*	323	372	*0.021*
villus width (µm)	94	92	*ns*	77	88	*ns*	80	87	*ns*	79	78	*ns*	83	87.5	*ns*	80	81	*ns*
Mucus-secreting (goblet) cells (cell/ villus)	8	9	*ns*	5	8	*ns*	7	17	*0.0002*	7	12	*0.024*	6	17	*<0,0001*	8	17	*0.0001*
Mucus vacuole diameter (µm)	7.8	9.8	*0.05*	8.3	9.2	*ns*	9.2	13.5	*0.0003*	8	11.7	*0.0056*	9	12.6	*0.0001*	9	12.4	*0.0001*
enterocyte length (µm)	25.6	28	*ns*	25	30	*0.008*	25	28	*0.0055*	23.5	27	*0.0016*	23	24.5	*ns*	22	25	*0.0006*
muscularis propria (µm)	35	45	*0.048*	32	46	*0.011*	41	74	*0.0003*	30	60	*<0,0001*	44.5	97	*<0,0001*	57	104	*<0.0001*
inner circular layer (µm)	21.6	28	*ns*	19	28	*0.003*	24	46	*0.0003*	18	39	*<0,0001*	26	64	*<0,0001*	33	70	*<0.0001*
ICL/MP (%)	62	63	*ns*	58.5	61	*ns*	58	62.5	*0.0274*	59.5	65	*0.005*	58	65	*0.0001*	58	67	*<0.0001*
outer longitudinal layer (µm)	13.6	17	*ns*	13	18	*0.056*	18	27.5	*0.0152*	11.5	21.5	*<0,0001*	19	34	*<0,0001*	23	34	*0.03*
OLL/MP (%)	36	38	*ns*	40.5	39	*ns*	41	37	*0.0464*	39	35	*0.0017*	42	35	*<0,0001*	41	33	*<0.0001*

	PC			C			DC		
Colon	WT	KO VIP	p	WT	KO VIP	p	WT	KO VIP	p
Number of animals (n)	9	5		4	4		4	4	
Average colon diameter (µm)	1699	1878	*ns*	1495	1626	*ns*	1527	1597	*ns*
macrovillus height (µm)	552	571	*ns*	488	510	*ns*	504	531	*ns*
mavrovillus widht (µm)	379	394	*ns*	329	378	*0.05*	389	409	*ns*

Small intestine	DU			D			PJ			J			DJ			IL		
	WT	KO VIP	p	WT	KO VIP	p	WT	KO VIP	p	WT	KO VIP	p	WT	KO VIP	p	WT	KO VIP	p
Number of animals (n)	**5**	**6**		**10**	**6**		**9**	**8**		**4**	**4**		**14**	**12**		**13**	**11**	
Microvillus height (μm)	209	219	*ns*	178	211	*0.003*	177	191	*ns*									
Microvillus width (μm)	54	54	*ns*	47	54	*0.05*	50	54	*ns*									
Enterocyte height (μm)	27	29	*ns*	23	28	*0.0037*	28	30	*ns*									
muscularis propria (μm)	123	147	*0.0047*	100	105	*ns*	108	116	*ns*									
inner circular layer (μm)	97.5	115	*0.04*	78.5	82	*ns*	77	82	*ns*									
ICL/MP (%)	79	78	*ns*	77	78	*ns*	71	71	*ns*									
outer longitudinal layer (μm)	24	27	*ns*	16	22	*ns*	31	34	*ns*									
OLL/MP (%)	20	21	*ns*	23	22	*ns*	29	29	*ns*									